



Synchronisation and Chaos in a Parametrically and Self-Excited System with Two Degrees of Freedom

JERZY WARMIŃSKI, GRZEGORZ LITAK, and KAZIMIERZ SZABELSKI

Department of Applied Mechanics, Technical University of Lublin, Nadbystrzycka 36 str., 20-618 Lublin, Poland

(Received: 17 April 1998; accepted: 6 October 1999)

Abstract. Vibration analysis of a non-linear parametrically and self-excited system of two degrees of freedom was carried out. The model contains two van der Pol oscillators coupled by a linear spring with a periodically changing stiffness of the Mathieu type. By means of a multiple-scales method, the existence and stability of periodic solutions close to the main parametric resonances have been investigated. Bifurcations of the system and regions of chaotic solutions have been found. The possibility of the appearance of hyperchaos has also been discussed and an example of such solution has been shown.

Keywords: Chaos, vibrations, self-excited system, parametric excitation.

1. Introduction

Vibrations described by differential equations with self-excited as well as with parametric excitation terms occur in some dynamic systems [1–5]. Systems with one degree of freedom have been studied by Tondl [1], Yano [2] and Szabelski and Warmiński [6, 7]. Such systems are interesting because they possess two different sources of vibration excitations. Thus, their characteristic features are a non-linear interaction between parametric and self-excitations and a synchronisation phenomenon. An entrainment of vibration takes place near the parametric resonances. In that region, systems vibrate periodically with only a single frequency. Outside the synchronisation area, almost-periodical vibrations appear, represented by almost periodic limit cycles on the Poincaré map or Hayashi plane [8]. One-degree-of-freedom systems of that broad class were found to vibrate chaotically for a wide range of system parameters [4, 5, 9]. Recently, systems with many degrees of freedom have attracted interest within the context of synchronisation phenomena [3] and chaotic vibrations [10, 13]. Many-degrees-of-freedom models can describe mechanical and electrical systems [1, 10–14]. One can also find them describing some mechanisms of vibrations generation in the case of manufacturing processes [15]. Among other aims, the study of hyperchaotic transitions has also been of interest [12, 13]. Unfortunately, papers [10–13] are only concerned with externally forced systems, so the results cannot be strictly generalised for parametric ones. In this paper, we examine vibrations of a two-degrees-of-freedom system with parametric and self-excitations. The paper is organised as follows: after a short introduction (Section 1) we present the physical model (Section 2). In Section 3 we provide analytic consideration by means of a multiple-scale-of-time method. Section 4 is devoted to synchronised vibrations near the main parametric resonances. In Section 5 bifurcations and chaotic vibrations are analysed while in Section 6 the possibility of the appearance of hyperchaos is briefly discussed. We end up with a summary and conclusions in Section 7.

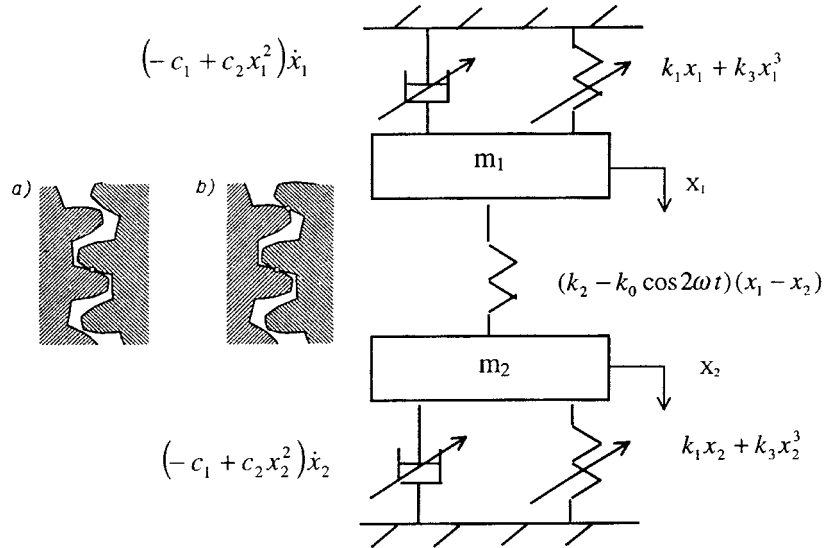


Figure 1. Physical model of the parametric self-excited system.

2. Vibrating System Model

Let us consider a parametric self-excited system with two degrees of freedom and non-linear symmetric characteristics of elasticity. The mathematical model consists of two van der Pol oscillators with Duffing terms. They are coupled by a linear spring with a periodically changing elasticity. Such a type of coupling occurs in descriptions of gear systems dynamics. In the first approximation, harmonic functions can be used to describe varying-in-time elasticity [16]. Schmidt [17] analysed a self-excitation of gears caused by breaking off the oil film between the meshing teeth. In our case, van der Pol terms are sources of self-excitation. The physical model of coupled oscillators is presented in Figure 1. Inserts (a) and (b) show different phases of gears, which correspond to varying elasticity.

Differential equations of motion in generalised co-ordinates have the following form:

$$\begin{aligned} m_1 x_1'' + (-c_1 + c_2 x_1^2) x_1' + k_1 x_1 + k_3 x_1^3 + (k_2 - k_0 \cos 2\omega t)(x_1 - x_2) &= 0, \\ m_2 x_2'' + (-c_1 + c_2 x_2^2) x_2' + k_1 x_2 + k_3 x_2^3 - (k_2 - k_0 \cos 2\omega t)(x_1 - x_2) &= 0. \end{aligned} \quad (1)$$

Introducing the non-dimensional time $\tau = \omega_1 t$; where $\omega_1 = \sqrt{k_1/m_1}$ and dependencies:

$$\begin{aligned} \vartheta &= \frac{\omega}{\omega_1}; & X_0 &= \frac{m_1 g}{k_1}; & \alpha_1 &= \frac{c_1}{m_1 \omega_1}; & \beta_1 &= \frac{c_2}{m_1 \omega_1} X_0^2; & \gamma_1 &= \frac{k_3}{m_1 \omega_1^2} X_0^2; \\ \delta_1 &= \frac{k_1}{m_1 \omega_1^2}; & \delta_2 &= \frac{k_2}{m_1 \omega_1^2}; & \mu &= \frac{k_0}{m_1 \omega_1^2}; & M &= \frac{m_1}{m_2}; & X_1 &= \frac{x_1}{X_0}; & X_2 &= \frac{x_2}{X_0}; \\ \dot{X}_1 &= \frac{dX_1}{d\tau}; & \ddot{X}_1 &= \frac{d^2 X_1}{d\tau^2}; & \dot{X}_2 &= \frac{dX_2}{d\tau}; & \ddot{X}_2 &= \frac{d^2 X_2}{d\tau^2}, \end{aligned}$$

dimensionless equations of motion can be written as

$$\begin{aligned}\ddot{X}_1 + (-\alpha_1 + \beta_1 X_1^2)\dot{X}_1 + \delta_1 X_1 + \gamma_1 X_1^3 + (\delta_2 - \mu \cos 2\vartheta\tau)(X_1 - X_2) &= 0, \\ \ddot{X}_2 + M(-\alpha_1 + \beta_1 X_2^2)\dot{X}_2 + M\delta_1 X_2 + M\gamma_1 X_2^3 - M(\delta_2 - \mu \cos 2\vartheta\tau)(X_1 - X_2) &= 0.\end{aligned}\quad (2)$$

Free vibration frequencies of the linear system are represented by the formula:

$$p_{1,2}^2 = \frac{1}{2}[(\delta_1 + \delta_2)(1 + M) \mp \sqrt{[(\delta_1 + \delta_2)(1 + M)]^2 - 4M\delta_1(\delta_1 + 2\delta_2)}]. \quad (3)$$

Including $\alpha_1 = \mu\tilde{\alpha}_1$; $\beta_1 = \mu\tilde{\beta}_1$; $\gamma_1 = \mu\tilde{\gamma}_1$ and introducing

$$Y_1 = X_1 + \lambda_1 X_2, \quad Y_2 = X_1 + \lambda_2 X_2, \quad (4)$$

we obtain differential equations in quasi-normal coordinates Y_1 and Y_2 :

$$\begin{aligned}\ddot{Y}_1 + p_1^2 Y_1 &= \mu \left\{ \begin{array}{l} -[-\tilde{\alpha}_1 + \tilde{\beta}_1(\Psi_1 Y_2 - \Psi_2 Y_1)^2](\Psi_1 \dot{Y}_2 - \Psi_2 \dot{Y}_1) \\ -M\lambda_1[-\tilde{\alpha}_1 + \tilde{\beta}_1\varphi^2(Y_1 - Y_2)^2]\varphi(\dot{Y}_1 - \dot{Y}_2) \\ +\tilde{\gamma}_1(\Psi_1 Y_2 - \Psi_2 Y_1)^3 - \tilde{\gamma}_1\lambda_1 M\varphi^3(Y_1 - Y_2)^3 \\ +\cos 2\vartheta\tau(Y_2\varepsilon_1 - Y_1\varepsilon_2)(1 - \lambda_1 M) \end{array} \right\}, \\ \ddot{Y}_2 + p_2^2 Y_2 &= \mu \left\{ \begin{array}{l} -[-\tilde{\alpha}_1 + \tilde{\beta}_1(\Psi_1 Y_2 - \Psi_2 Y_1)^2](\Psi_1 \dot{Y}_2 - \Psi_2 \dot{Y}_1) \\ -M\lambda_2[-\tilde{\alpha}_1 + \tilde{\beta}_1\varphi^2(Y_1 - Y_2)^2]\varphi(\dot{Y}_1 - \dot{Y}_2) \\ -\tilde{\gamma}_1(\Psi_1 Y_2 - \Psi_2 Y_1)^3 - \tilde{\gamma}_1\lambda_2 M\varphi^3(Y_1 - Y_2)^3 \\ +\cos 2\vartheta\tau(Y_2\varepsilon_1 - Y_1\varepsilon_2)(1 - \lambda_2 M) \end{array} \right\}.\end{aligned}\quad (5)$$

In the transformation of coordinates, the following notation is introduced:

$$\begin{aligned}\lambda_1 &= \frac{\delta_1 + \delta_2 - p_1^2}{\delta_2 M}; \quad \lambda_2 = \frac{\delta_1 + \delta_2 - p_2^2}{\delta_2 M}; \quad \varphi = \frac{1}{\lambda_1 - \lambda_2}; \\ \psi_1 &= \frac{\lambda_1}{\lambda_1 - \lambda_2}; \quad \psi_2 = \frac{\lambda_2}{\lambda_1 - \lambda_2}; \quad \varepsilon_1 = \Psi_1 + \varphi; \quad \varepsilon_2 = \Psi_2 + \varphi.\end{aligned}$$

For $\mu = 0$, the system of equations is decoupled into two independent differential equations. Generally, different types of resonance can appear in a system with many degrees of freedom [18] and harmonic resonances, as well as internal and combination ones, can be taken into account. For the internal resonance, the free frequencies must satisfy the condition

$$\sum_{i=1}^s n_i p_i = 0; \quad i = 1, 2, \dots, s; \quad s \leq N,$$

where n_i is the integer number, N the number of degrees of freedom, s a natural number, and p_i the free frequency of the system. In the case of two degrees of freedom, the above condition reads:

$$n_1 p_1 + n_2 p_2 = 0.$$

If a parametric excitation frequency ϑ is close to one of free frequencies, a solution needs both quasi-normal coordinates to be considered simultaneously.

On the other hand, the condition for a combination resonance existence can be written as $n\vartheta = \sum_{i=1}^s n_i p_i$, where n denotes a natural number. In the case of a two-degrees-of-freedom system, a combination resonance can often be met in a region between two natural frequencies.

3. Analytical Examinations

The examinations of parametric and self-excited systems were carried out by applying various approximate analytical methods [1, 3]. We anticipate a periodic solution of Equation (5) using the multiple-scale-of-time method [14]. For analytical calculations, μ is used as a small parameter. In a real mechanical system, the modulation of stiffness μ is rather small in comparison with its average value δ_2 . We define different time scales $T_n = \mu^n \tau$, $n = 0, 1, 2, \dots$. In the case of the main parametric resonance close to the first frequency of the free vibrations, we can write

$$\vartheta^2 = p_1^2 + \mu\sigma_1. \quad (6)$$

Solutions of the system in Equations (5) are anticipated in form

$$\begin{aligned} Y_1(\tau; \mu) &= Y_{10}(T_0, T_1) + \mu Y_{11}(T_0, T_1) + \dots, \\ Y_2(\tau; \mu) &= \mu Y_{21}(T_0, T_1) + \dots. \end{aligned} \quad (7)$$

Time derivatives are expressed by the formulae:

$$\frac{d}{d\tau} = D_0 + \mu D_1 + \dots, \quad \frac{d^2}{d\tau^2} = D_0^2 + 2\mu D_0 D_1 + \dots,$$

where $D_n^m = \partial^m / \partial T_n^m$. Applying expressions (7) and (6) to Equation (5), we obtain

$$D_0^2 Y_{10} + \vartheta^2 Y_{10} = 0 \quad (8)$$

$$\begin{aligned} D_0^2 Y_{11} + \vartheta^2 Y_{11} &= -2D_0 D_1 Y_{10} + \tilde{\alpha}_1 (M\lambda_1 \varphi - \Psi_2) D_0 Y_{10} \\ &\quad - \tilde{\beta}_1 Y_{10}^2 (\Psi_2^3 - M\lambda_1 \varphi^3) D_0 Y_{10} \\ &\quad + \sigma_1 Y_{10} - \varepsilon_2 Y_{10} (1 - \lambda_1 M) \cos 2\vartheta\tau + (\Psi_2^3 - M\lambda_1 \varphi^3) \tilde{\gamma}_1 Y_{10}^3. \end{aligned} \quad (9)$$

The solution of Equation (8) may be presented in the form

$$Y_{10}(T_0, T_1) = A(T_1) \exp(i\vartheta T_0) + \bar{A}(T_1) \exp(-i\vartheta T_0). \quad (10)$$

Putting (10) into (9), we get

$$\begin{aligned} D_0^2 Y_{10} + \vartheta^2 Y_{10} &= \left[-2i\vartheta D_1 A + (\sigma_1 + \alpha_1 (M\lambda_1 \varphi - \Psi_2) i\vartheta) A \right. \\ &\quad \left. + (\beta_1 (\Psi_2^3 - M\lambda_1 \varphi^3) i\vartheta - 3\gamma_1 (\Psi_2^3 - M\lambda_1 \varphi^3)) A^2 \bar{A} - \frac{1}{2} \varepsilon_2 \left(1 - \frac{1}{2} M\lambda_1 \right) \bar{A} \right] \exp(i\vartheta T_0) \\ &\quad \left. + \left[-\frac{1}{2} \varepsilon_2 (1 - M\lambda_1) A + (\tilde{\gamma} + i\tilde{\beta}_1 \vartheta) (\Psi_2^3 - M\lambda_1 \varphi^3) A^3 \right] \exp(3i\vartheta T_0) + \text{c.c.} \end{aligned} \quad (11)$$

The condition for the elimination of secular terms leads to the relation:

$$\begin{aligned}
 -2i\vartheta D_1 A + (\sigma_1 + \tilde{\alpha}_1(M\lambda_1\varphi - \Psi_2)i\vartheta)A \\
 + (\tilde{\beta}_1(\Psi_2^3 - M\lambda_1\varphi^3)i\vartheta - 3\tilde{\gamma}_1(\Psi_2^3 - M\lambda_1\varphi^3))A^2\bar{A} \\
 - \frac{1}{2}\varepsilon_2\left(1 - \frac{1}{2}M\lambda_1\right)\bar{A} = 0.
 \end{aligned} \tag{12}$$

The function A is expressed by the formula

$$A = \frac{1}{2}a(\tau) \exp[i\Phi(\tau)]. \tag{13}$$

After substituting (13) into (12) and separating the real and imaginary parts, we find

$$\begin{aligned}
 \dot{a} &= \frac{\tilde{\alpha}_1(M\lambda_1\varphi - \Psi_2)}{2}a + \frac{\tilde{\beta}_1(\Psi_2^3 - M\lambda_1\varphi^3)}{8}a^3 + \frac{\varepsilon_2}{4\vartheta}(1 - M\lambda_1)a \sin(2\Phi), \\
 a\dot{\Phi} &= -\frac{\sigma_1}{2\vartheta}a - \frac{3\tilde{\gamma}_1(\Psi_2^3 - M\lambda_1\varphi^3)}{8\vartheta}a^3 + \frac{\varepsilon_2}{4\vartheta}(1 - M\lambda_1)a \cos(2\Phi).
 \end{aligned} \tag{14}$$

A solution in a first-order approximation has the form:

$$Y_1(t) = a \cos(\vartheta t + \Phi) + \dots \tag{15}$$

For the stationary state $\dot{a} = 0$; $\dot{\Phi} = 0$, we obtain the following system of algebraic non-linear equations:

$$\begin{aligned}
 \frac{\tilde{\alpha}_1(M\lambda_1\varphi - \Psi_2)}{2} + \frac{\tilde{\beta}_1(\Psi_2^3 - M\lambda_1\varphi^3)}{8}a^2 + \frac{\varepsilon_2}{4\vartheta}(1 - M\lambda_1) \sin(2\Phi) = 0, \\
 -\frac{\sigma_1}{2\vartheta} - \frac{3\tilde{\gamma}_1(\Psi_2^3 - M\lambda_1\varphi^3)}{8\vartheta}a^2 + \frac{\varepsilon_2}{4\vartheta}(1 - M\lambda_1) \cos(2\Phi) = 0.
 \end{aligned} \tag{16}$$

Using (6) and (16), we obtain an equation for determining the amplitude of a periodic solution:

$$\begin{aligned}
 \frac{1}{8}(M\lambda_1\varphi^3 - \Psi_2^3)[9\tilde{\gamma}_1^2(M\lambda_1\varphi^3 - \Psi_2^3) + \tilde{\beta}_1^2\vartheta^2]a^4 \\
 + \tilde{\alpha}_1\tilde{\beta}_1[-M^2\lambda_1^2\varphi^4 + M\lambda_1\Psi_2\varphi^3(1 + \Psi_2^2) - \Psi_2^4]\vartheta^2a^2 \\
 + \left[-\frac{1}{2} + M\lambda_1\left(1 - \frac{1}{2}M^2\lambda_1^2\right)\right]\varepsilon_2^2 + \frac{2}{\mu}(\vartheta^2 - p_1^2)^2 \\
 + 2\tilde{\alpha}_1^2(M\lambda_1\varphi - \Psi_2)^2\vartheta^2 + \frac{3\tilde{\gamma}_1}{\mu}[(M\lambda_1\varphi^3 - \Psi_2^3)(p_1^2 - \vartheta^2)] = 0.
 \end{aligned} \tag{17}$$

Equation (17) can have trivial ($a = 0$) and non-trivial ($a \neq 0$) solutions. By putting $a = 0$ into (17) we obtain:

$$\vartheta^4 + \alpha_1^2 \left[(M\lambda_1\varphi - \Psi_2)^2 - \frac{4p_1^2}{\mu^2} \right] \vartheta^2 - \frac{1}{4}\mu^2\varepsilon_2^2(1 - M\lambda_1)^2 + p_1^4 = 0$$

and bifurcation points

$$\vartheta_{1,2}^* = \sqrt{\frac{1}{2} \left| -\alpha_1^2 \left[(M\lambda_1\varphi - \Psi_2)^2 - \frac{4p_1^2}{\mu^2} \right] \mp \sqrt{\alpha_1^4 \left[(M\lambda_1\varphi - \Psi_2)^2 - \frac{4p_1^2}{\mu^2} \right]^2 + \mu^2 \varepsilon_2^2 (1 - M\lambda_1)^2 - 4p_1^4} \right|}. \quad (18)$$

Parameters $\vartheta_{1,2}^*$ define the points of curve $a(\vartheta)$ which lie on ϑ axis ($a(\vartheta) = 0$). These points can appear when the following condition is satisfied:

$$|\tilde{\alpha}_1| \langle \sim \left| \frac{\varepsilon_2(1 - M\lambda_1)}{2p_1(M\lambda_1\varphi - \Psi_2)} \right|. \quad (19)$$

In the case of resonance with respect to the second frequency of free vibrations, we can write

$$\vartheta^2 = p_2^2 + \mu\sigma_2 \quad (20)$$

and we anticipate the solution of Equations (5) in the following form:

$$Y_1(\tau; \mu) = \mu Y_{11}(T_0, T_1) + \dots,$$

$$Y_2(\tau; \mu) = Y_{20}(T_0, T_1) + \mu Y_{21}(T_0, T_1) + \dots. \quad (21)$$

Applying a similar procedure, as in the previous case (6–14), we obtain two differential equations of the first order:

$$\begin{aligned} \dot{a} &= \frac{-\tilde{\alpha}_1(M\lambda_2\varphi - \Psi_1)}{2}a - \frac{\tilde{\beta}_1(\Psi_1^3 - M\lambda_2\varphi^3)}{8}a^3 - \frac{\varepsilon_1}{4\vartheta}(1 - M\lambda_2)a \sin(2\Phi), \\ a\dot{\Phi} &= -\frac{\sigma_2}{2\vartheta}a + \frac{3\tilde{\gamma}_1(\Psi_1^3 - M\lambda_2\varphi^3)}{8\vartheta}a^3 - \frac{\varepsilon_1}{4\vartheta}(1 - M\lambda_2)a \cos(2\Phi). \end{aligned} \quad (22)$$

A solution in a first-order approximation has the form:

$$Y_2(t) = a \cos(\vartheta t + \Phi) + \dots. \quad (23)$$

The stationary state is described by the dependence:

$$\begin{aligned} &\frac{1}{8}(M\lambda_2\varphi^3 - \Psi_1^3)[9\tilde{\gamma}_1^2(M\lambda_2\varphi^3 - \Psi_1^3) + \tilde{\beta}_1^2\vartheta^2]a^4 \\ &+ \tilde{\alpha}_1\tilde{\beta}_1[-M^2\lambda_2^2\varphi^4 + M\lambda_2\Psi_1\varphi^3(1 + \Psi_1^2) - \Psi_1^4]\vartheta^2a^2 \\ &+ \left[-\frac{1}{2} + M\lambda_2 \left(1 - \frac{1}{2}M^2\lambda_2^2 \right) \right] \varepsilon_1^2 + \frac{2}{\mu}(\vartheta^2 - p_2^2)^2 \\ &+ 2\tilde{\alpha}_1^2(M\lambda_2\varphi - \Psi_1)^2\vartheta^2 + \frac{3\tilde{\gamma}_1}{\mu}[(M\lambda_2\varphi^3 - \Psi_1^3)(p_2^2 - \vartheta^2)] = 0. \end{aligned} \quad (24)$$

Bifurcation points of trivial and non-trivial solutions can be obtained from the formula:

$$\vartheta_{1,2}^* = \sqrt{\frac{1}{2} \left| -\alpha_1^2 \left[(M\lambda_2\varphi - \Psi_1)^2 - \frac{4p_2^2}{\mu^2} \right] \mp \sqrt{\alpha_1^4 \left[(M\lambda_2\varphi - \Psi_1)^2 - \frac{4p_2^2}{\mu^2} \right]^2 + \mu^2 \varepsilon_1^2 (1 - M\lambda_2)^2 - 4p_2^4} \right|}. \quad (25)$$

and then:

$$|\tilde{\alpha}| \langle \sim \left| \frac{\varepsilon_1(1 - M\lambda_2)}{2p_2(M\lambda_2\varphi - \Psi_1)} \right|. \quad (26)$$

The stability of periodic solutions will be carried out using approximate differential equations of the first order (14) and (22) in a shortened form:

$$\dot{a} = f_1(a, \Phi); \quad \dot{\Phi} = f_2(a, \Phi). \quad (27)$$

For such equations, the characteristic determinant of the variational system has the following form:

$$\begin{vmatrix} \left(\frac{\partial f_1}{\partial a}\right)_0 - \rho & \left(\frac{\partial f_1}{\partial \Phi}\right)_0 \\ \left(\frac{\partial f_2}{\partial a}\right)_0 & \left(\frac{\partial f_2}{\partial \Phi}\right)_0 - \rho \end{vmatrix} = 0. \quad (28)$$

Index '0' denotes partial derivatives in the equilibrium point. The stability of the approximate solution depends on the roots of the characteristic equation (28), which are determined by

$$\rho_{1,2} = \frac{1}{2}(-q_1 \mp \sqrt{q_1^2 - 4q_2}), \quad (29)$$

where, for the main parametric resonance with respect to the frequency p_1 ,

$$\begin{aligned} q_1 &= \frac{1}{2}\tilde{\alpha}_1[\Psi_2 - M\lambda_1\varphi] + \frac{3}{8}\tilde{\beta}_1(M\lambda_1\varphi^3 - \Psi_2^3)a^2 + \frac{1}{4}\frac{\varepsilon_2}{\vartheta}(1 - M\lambda_1)\sin 2\Phi, \\ q_2 &= \left[\frac{1}{4}\tilde{\alpha}_1\frac{\varepsilon_2}{\vartheta}(\Psi_2 - M\lambda_1\varphi) + \frac{3}{16}\tilde{\beta}_1\varepsilon_2\frac{a^2}{\vartheta}(M\lambda_1\varphi^3 - \Psi_2^3) \right] \cdot (1 - M\lambda_1)\sin 2\Phi \\ &\quad + \frac{3}{8}\tilde{\gamma}_1\varepsilon_2\frac{a^2}{\vartheta^2}(\Psi_2^3 - M\lambda_1\varphi^3) \cdot (1 - M\lambda_1)\cos 2\Phi - \frac{1}{8}\frac{\varepsilon_2^2}{\vartheta^2}(1 - M\lambda_1)^2\sin^2 2\Phi \end{aligned} \quad (30)$$

and for the main parametric resonance with respect to the frequency p_2 ,

$$\begin{aligned} q_1 &= -\frac{1}{2}\tilde{\alpha}_1[\Psi_1 - M\lambda_2\varphi] - \frac{3}{8}\tilde{\beta}_1(M\lambda_2\varphi^3 - \Psi_1^3)a^2 - \frac{1}{4}\frac{\varepsilon_1}{\vartheta}(1 - M\lambda_2)\sin 2\Phi, \\ q_2 &= \left[-\frac{1}{4}\tilde{\alpha}_1\frac{\varepsilon_1}{\vartheta}(\Psi_1 - M\lambda_2\varphi) - \frac{3}{16}\tilde{\beta}_1\varepsilon_1\frac{a^2}{\vartheta}(M\lambda_2\varphi^3 - \Psi_1^3) \right] \cdot (1 - M\lambda_2)\sin 2\Phi \\ &\quad - \frac{3}{8}\tilde{\gamma}_1\varepsilon_1\frac{a^2}{\vartheta^2}(\Psi_1^3 - M\lambda_2\varphi^3) \cdot (1 - M\lambda_2)\cos 2\Phi + \frac{1}{8}\frac{\varepsilon_1^2}{\vartheta^2}(1 - M\lambda_2)^2\sin^2 2\Phi. \end{aligned} \quad (31)$$

The stability condition will be satisfied when all characteristic equation roots of the first-order approximation system have negative real terms.

4. Regular Vibrations

The example calculations were carried out by using derived analytical dependencies and numerical simulations. For numerical examinations, we have used the 'Dynamics' package [19] as well as our Fortran procedures. Calculations were done for different sets of system

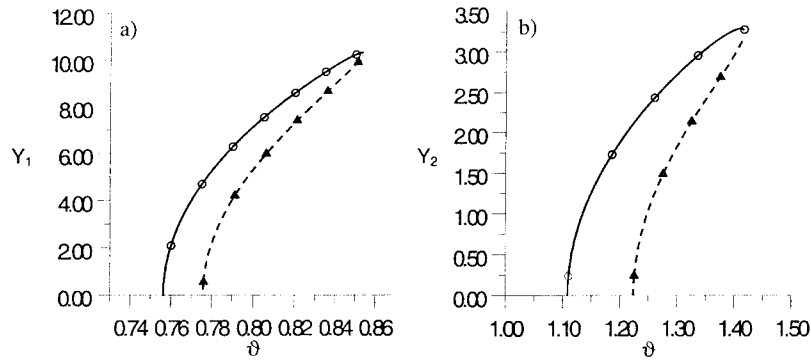


Figure 2. Main parametric resonance around the first (a) and second (b) frequencies of the system-free vibrations; $-o-o-$ stable focus; $-\Delta-\Delta-$ unstable saddle.

parameters taken from the most interesting intervals of physical systems [1, 2]. Sample results of calculations were obtained for the following parameters:

$$\alpha_1 = 0.01, \quad \beta_1 = 0.05, \quad \gamma_1 = 0.1, \quad \mu = 0.2, \quad M = 0.5, \quad \delta_1 = 1.0, \quad \delta_2 = 0.3. \quad (32)$$

Transformation from the generalised (Equations (2)) to quasi-normal coordinates (Equations (5)) demands, bearing in mind the relationships given in Section 2, determining the free vibrations frequencies p_1, p_2 of a linear system and values of the coefficients $\lambda_1, \lambda_2, \varphi, \Psi_1, \Psi_2, \varepsilon_1, \varepsilon_2$. These values are

$$p_1 = 0.766, \quad p_2 = 1.168, \quad \lambda_1 = 4.754, \quad \lambda_2 = -0.421, \\ \varphi = 0.193, \quad \Psi_1 = 0.919, \quad \Psi_2 = -0.0813, \quad \varepsilon_1 = 1.112, \quad \varepsilon_2 = 0.112.$$

For the accepted values of the set of system parameters, the resonance curve around the first (p_1) and the second (p_2) of free vibration frequencies were plotted in Figures 2a and 2b, respectively. The figures present amplitudes of vibrations in quasi-normal coordinates. The solid line means the stable periodic solution and the dashed one means the unstable solution. The stability type was checked according to the characteristic equation roots (29). We obtained two types of stability: stable focus marked by a circle (complex roots with a negative real part) and unstable saddle point marked by a triangle (two real roots, one negative and one positive). We also calculated the bifurcation points of both trivial and non-trivial solutions. For p_1 we obtained $\vartheta_1^* = 0.756$ and $\vartheta_2^* = 0.776$ from (18), satisfying the condition (19) $\tilde{\alpha}_1 = 0.05 < 0.186$, and for p_2 from (25) $\vartheta_1^* = 1.109$ and $\vartheta_2^* = 1.224$ with the condition (26) $\tilde{\alpha}_1 = 0.05 < 179.875$, respectively.

In Figure 3, we present the numerical results as a bifurcation diagram for the analysed system parameters (32). X_1 was plotted in a stroboscopic way with an excitation frequency. Here one can see two regions of the discussed main parametric resonances for $\vartheta \in [0.78; 0.85]$ and $\vartheta \in [1.15; 1.40]$, respectively. It is also possible to observe a combination resonance in the middle of these two regions. There is also an additional resonance for very low frequency $\vartheta \approx 0.6$, which, however, was not analysed analytically in this paper. On the other hand, for a symmetric system (parameters are chosen as in (32) but $M = 1.0$ and $\delta_2 = 1.0$) we found that condition (18) for the first frequency of free vibration $p_1 = 1.0$, is not fulfilled. Thus, instead of two regions of main resonance, only one region around $p_2 = 1.73$ is present.

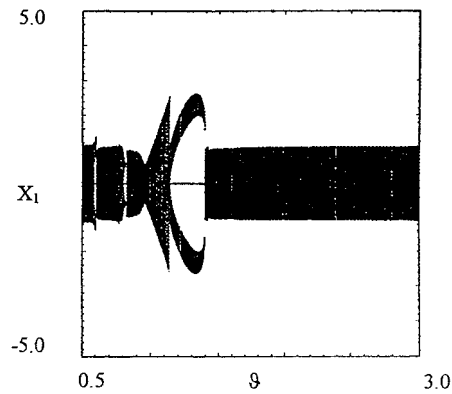


Figure 3. Bifurcation diagram versus ϑ for the system parameters (32).

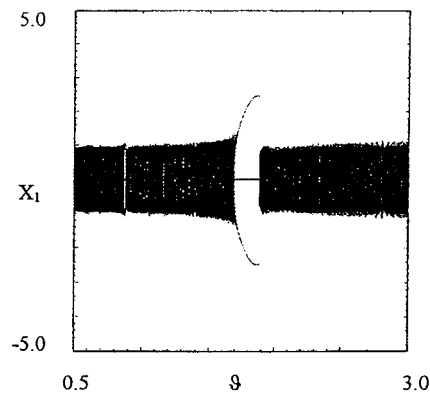


Figure 4. Bifurcation diagram versus ϑ parameter for a symmetric system ($M = 1.0$, $\delta_2 = 1.0$).

Figure 4 shows a bifurcation diagram for these parameters. In the figure, only one region for $\vartheta \in [1.7, 1.9]$ with synchronised vibration is visible. Note that in the generalised coordinates, the synchronisation is not clearly manifested (Figure 3) as it usually is observed in one-degree-of-freedom systems [4, 6–9]. In Figures 5a–5d, we present time histories for the system parameters (32) and $\vartheta = 0.80$ both for quasi-normal (Figures 5a, 5b) and for generalised (Figures 5c, 5d) coordinates.

The solution expressed in quasi-normal coordinates allows us to analyse the complex system as two independent systems with one degree of freedom. It is a general feature of a multi-degrees-of-freedom system with small non-linearities. In the case of a two-degrees-of-freedom system, the vibrations are often characterised by two frequencies and they are decoupled in quasi-normal coordinates, assuming a small μ parameter. The small modulations of a vibration amplitude visible in Figures 5a and 5b are due to the non-linearities of the considered system. In the case of a symmetric system (Figure 4), there is only one characteristic frequency, $p_2 = 1.73$, and the vibrations are of single frequency for both quasi-normal and generalised coordinates.

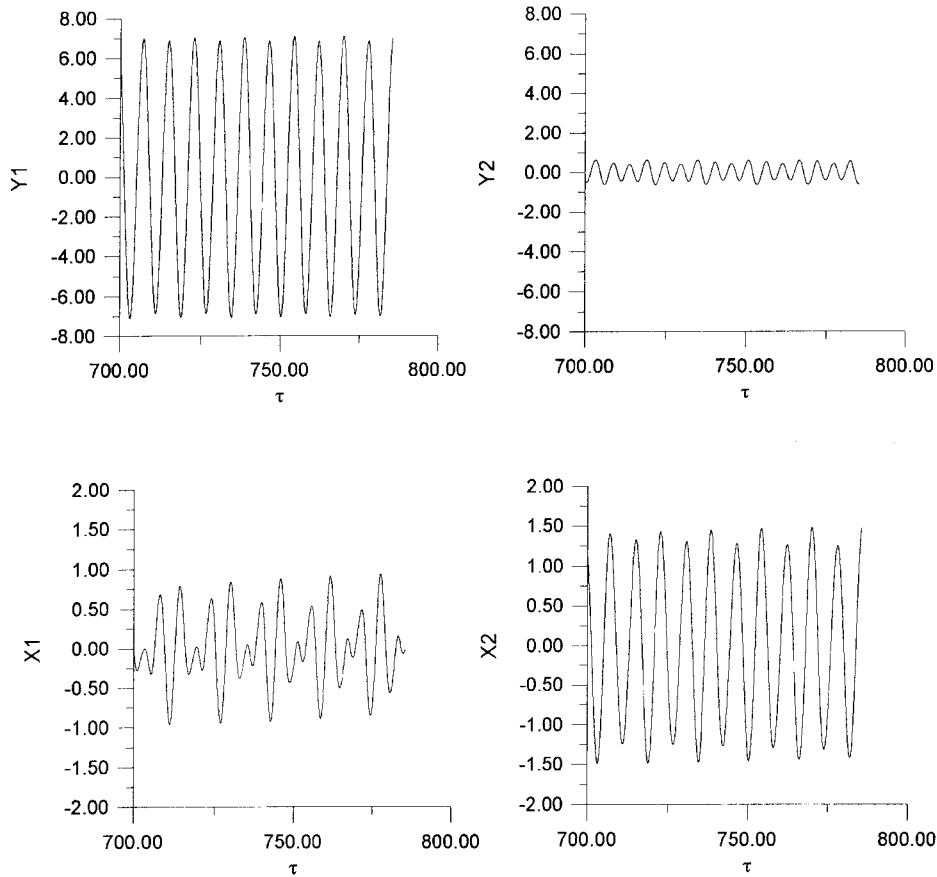


Figure 5. Vibration time histories in quasi-normal (a, b) and generalised (c, d) coordinates around p_1 frequency for $\vartheta = 0.80$.

5. Bifurcations and Chaotic Vibrations

We have transformed two second-order differential equations (Equation (2)) into a system of four first-order differential equations and have simulated them numerically. Using the same system parameters as (32), but with larger excitation amplitude μ :

$$\alpha_1 = 0.01, \quad \beta_1 = 0.05, \quad \gamma_1 = 0.1, \quad \delta_1 = 1.0, \quad \delta_2 = 0.3, \quad \mu = 0.8, \quad M = 0.5, \quad (33)$$

we have calculated the maximal Lyapunov exponent λ (we do not consider the additional nodal exponent which always appears in a non-autonomous system) in the region of excitation frequency $\vartheta \in [0.5, 2.5]$. The exponent has been calculated six times for different initial conditions and plotted *versus* ϑ in Figure 6. The picture shows that three regions of positive values of the Lyapunov exponent are present around $\vartheta \cong 0.56, 0.95$ and in an interval $\vartheta \in [1.38, 1.51]$. These regions correspond to the chaotic behaviour of the system. Apart from that, the majority of solutions are associated with $\lambda \approx 0.00$ (Figure 6).

Such a value of the Lyapunov exponent is usually connected with a quasi-periodic solution or a bifurcation point. For relatively small values of excitation frequency $\vartheta \in [0.5, 0.6]$ and $\vartheta \in [0.8, 1.0]$ (and some singular points around $\vartheta \cong 1.5$), we see a definite negative value of

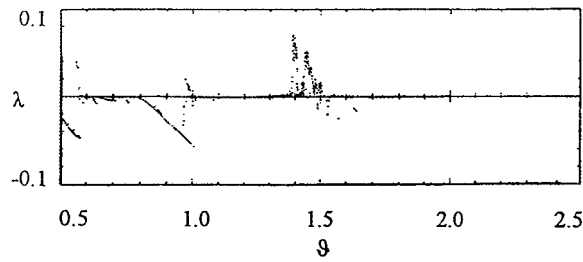


Figure 6. Lyapunov exponent versus ϑ parameter.

λ . This corresponds to the regular solution synchronised with parametric excitation. In many regions, we found a number of possible values of λ , where for the same system parameters but different initial conditions, solutions of such different types as periodic, quasi-periodic and chaotic, can coexist. For clarity, we have analysed the evolution of attractors by means of a Poincaré map. Figure 7 presents the Poincaré maps for the same set of parameters as in Figure 6 (33) and some chosen values of ϑ . In Figure 7a ($\vartheta = 0.56$), we show one strange chaotic attractor (denoted by 3) and two other regular solutions synchronised with excitation (denoted by 2 and 3), each represented by three singular points. For the larger value of $\vartheta = 0.7$ (Figure 7b), we observe one quasi-periodic attractor (denoted by 1) and two regular periodic attractors (denoted by 2, 3). Figure 7c ($\vartheta = 98$) shows again one chaotic (denoted by 1) and two regular periodic attractors (denoted by 2, 3). For $\vartheta = 1.1$ (Figure 7d), we have found only one quasi-periodic attractor with a close curve on the Poincaré map. For $\vartheta = 1.4$ (Figure 7e), a quasi-periodic motion transits to a chaotic one which is represented by a strange attractor and, later, this large strange attractor splits into two chaotic motions (denoted by 2 and 3 in Figure 7f) with an additional quasi-periodic attractor in the middle of Figure 7f (denoted by 1). In Figure 7g ($\vartheta = 1.7$), one can see that a quasi-periodic solution is still present in the middle of the picture (denoted by 1) but two others have changed into other quasi-periodic solutions (denoted by 2 and 3).

Using this analysis for larger value of ϑ , we obtained one quasi-periodic attractor of a different topology represented by a singular closed curve (Figure 7h). However, for larger excitation frequencies $\vartheta = 1.9$ and $\vartheta = 2.5$, we note that the quasi-periodic attractors (Figures 7i and 7j) resemble a structure similar to the quasi-periodic one (denoted by 1) in Figure 7g. For each of the cases examined, we have calculated all non-trivial Lyapunov exponents and expressed them in Table 1. Analysing the table, one can see that some of the quasi-periodic solutions have only one nodal Lyapunov, exponent while the others have even two nodal values. Attractors with a closed curve on Poincaré maps (Figures 7d, 7g (2, 3), 7h) have only one nodal Lyapunov exponent but attractors represented by torus structures on Poincaré maps (Figures 7b (1), 7f(1), g(1), i, j) are characterised by two nodal Lyapunov exponents (Table 1). The change of attractor topology with changing ϑ can be interpreted as Hopf bifurcation [20].

Figure 8 presents a bifurcation diagram of X_1 against ϑ for the examined system. For each value of ϑ , the calculations were repeated six times for different sets of initial conditions. One can easily recognise the synchronised periodic motions of the system represented by singular lines in the diagram. However, it is rather difficult to distinguish quasi-periodic solutions from chaotic ones. This is because they are similarly represented in the figure by black regions. This bifurcation diagram is much richer than the former for smaller value of the excitation amplitude

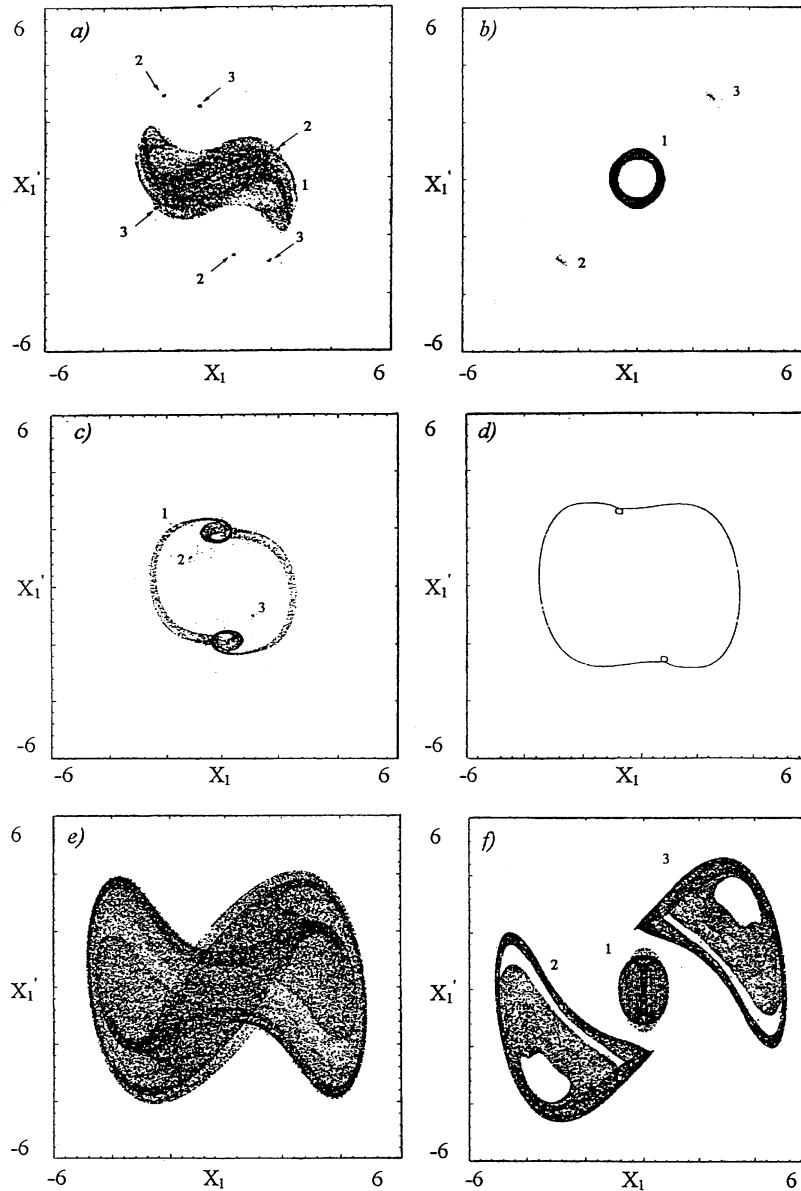


Figure 7. Poincaré maps for various values of ϑ . (a) $\vartheta = 0.56$; (b) $\vartheta = 0.70$; (c) $\vartheta = 0.98$; (d) $\vartheta = 1.10$; (e) $\vartheta = 1.40$; (f) $\vartheta = 1.50$.

$\mu = 0.2$ (Figure 3). For comparison, we have done the numerical calculations for a much larger excitation amplitude μ . In Figure 9, the maximal Lyapunov exponent was plotted *versus* ϑ for the system parameters assumed to be like (33) but for $\mu = 10.0$. For most of the frequencies ϑ , the Lyapunov exponent is negative. Nevertheless, we have observed three clear regions of negative values of λ around $\vartheta = 0.58$ and $\vartheta = 0.92$ and the interval $\vartheta \in [1.39, 1.55]$. Interestingly, they closely correspond to three similar regions of chaotic solutions obtained for a smaller value of excitation amplitude, $\mu = 0.8$ (Figure 6). For $1.8 < \vartheta < 2.5$, the Lyapunov exponent is negative and smaller than -1.0 (beyond the range of the diagram in

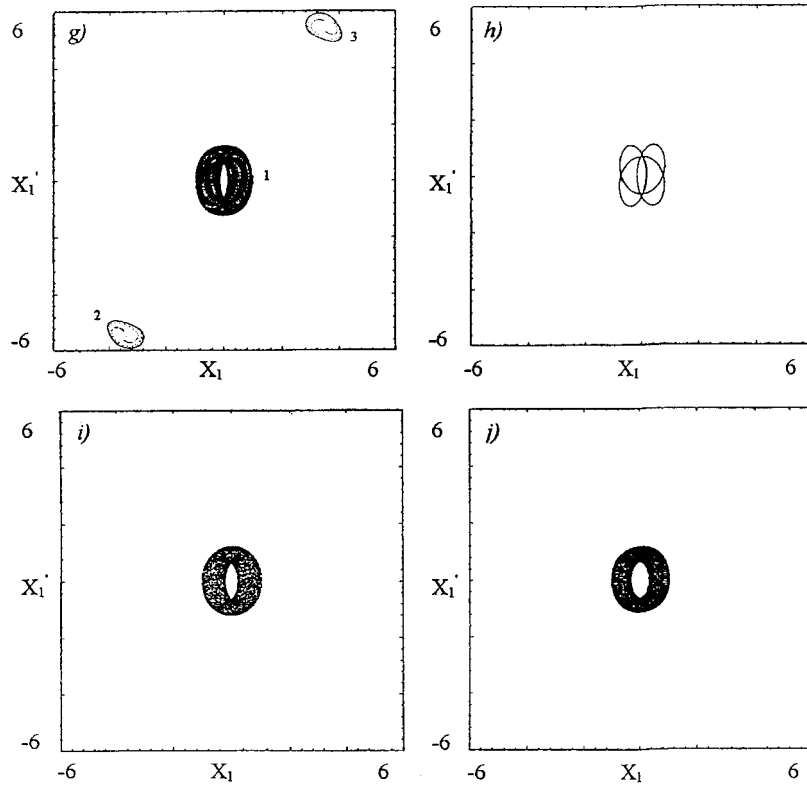


Figure 7. Continued. (g) $\vartheta = 1.70$; (h) $\vartheta = 1.80$; (i) $\vartheta = 1.90$; (j) $\vartheta = 2.50$.

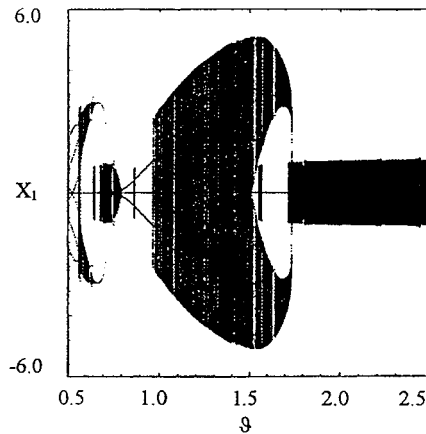


Figure 8. Bifurcation diagram versus ϑ . System parameters as in Figure 6.

Figure 9). Note the scale in Figure 9 is different from that in Figure 6. The main difference between these two diagrams is that the positive value of the Lyapunov exponent is much larger (three times larger) for $\mu = 10.0$ than for $\mu = 0.8$ (Figure 6 and Table 1). The large range of Lyapunov exponent fluctuations visible in Figure 9 is obviously connected with the large value of the parametric excitation amplitude μ . Figure 10 shows examples of Poincaré maps for a number of excitation frequencies. Starting from $\vartheta = 0.98$, we find two periodic attractors

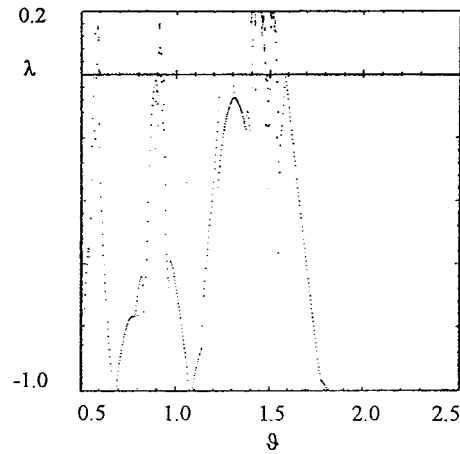


Figure 9. Maximal Lyapunov exponent versus ϑ . System parameters as in Figure 6 but $\mu = 10$.

Table 1. Lyapunov exponents for various ϑ parameters.

| ϑ | Attractor type (see in Figures 7a–7j) | λ_1 | λ_2 | λ_3 | λ_4 |
|-------------|--|-------------|-------------|-------------|-------------|
| 0.56 | Chaotic – No. 1 | 0.037 | –0.004 | –0.019 | –0.094 |
| 0.56 | Periodic – No. 2, 3 | –0.044 | –0.045 | –0.073 | –0.073 |
| 0.70 | Quasi-periodic – No. 1 | 0.000 | 0.000 | –0.003 | –0.009 |
| 0.70 | Periodic – No. 2, 3 | –0.005 | –0.005 | –0.124 | –0.124 |
| 0.98 | Chaotic – No. 1 | 0.012 | –0.001 | –0.066 | –0.124 |
| 0.98 | Periodic – No. 2, 3 | –0.050 | –0.051 | –0.057 | –0.059 |
| 1.10 | Quasi-periodic | 0.000 | –0.075 | –0.075 | –0.170 |
| 1.40 | Chaotic | 0.049 | 0.000 | –0.138 | –0.260 |
| 1.50 | Quasi-periodic – No. 1 | 0.000 | 0.000 | –0.002 | –0.007 |
| 1.50 | Chaotic – No. 2, 3 | 0.013 | 0.001 | –0.120 | –0.322 |
| 1.70 | Quasi-periodic – No. 1 | 0.000 | 0.000 | –0.002 | –0.007 |
| 1.70 | Quasi-periodic – No. 2, 3 | 0.000 | –0.018 | –0.266 | –0.266 |
| 1.80 | Quasi-periodic | 0.000 | –0.002 | –0.003 | –0.003 |
| 1.90 | Quasi-periodic | 0.000 | 0.000 | –0.002 | –0.007 |
| 2.50 | Quasi-periodic | 0.000 | 0.000 | –0.003 | –0.007 |

with a single frequency (denoted by 1 and 2 in Figure 10a). For $\vartheta = 1.4$ and $\vartheta = 1.5$, we have found chaotic motions of the system, represented by strange attractors in Figures 10b and 10c. It is interesting to note that the strange attractor visible in Figure 10b is split into two separate strange attractors (denoted 1 and 2 and obtained for different initial conditions). Figure 10d presents again two periodic solutions with a single frequency. All four non-trivial Lyapunov exponents calculated for the considered cases ($\vartheta = 0.98, 1.40, 1.50, 1.70$) are given in Table 2. Figure 11 shows a bifurcation diagram plotted against excitation frequency for $\mu = 10$. We can easily recognise the regions of periodic and chaotic motions, which

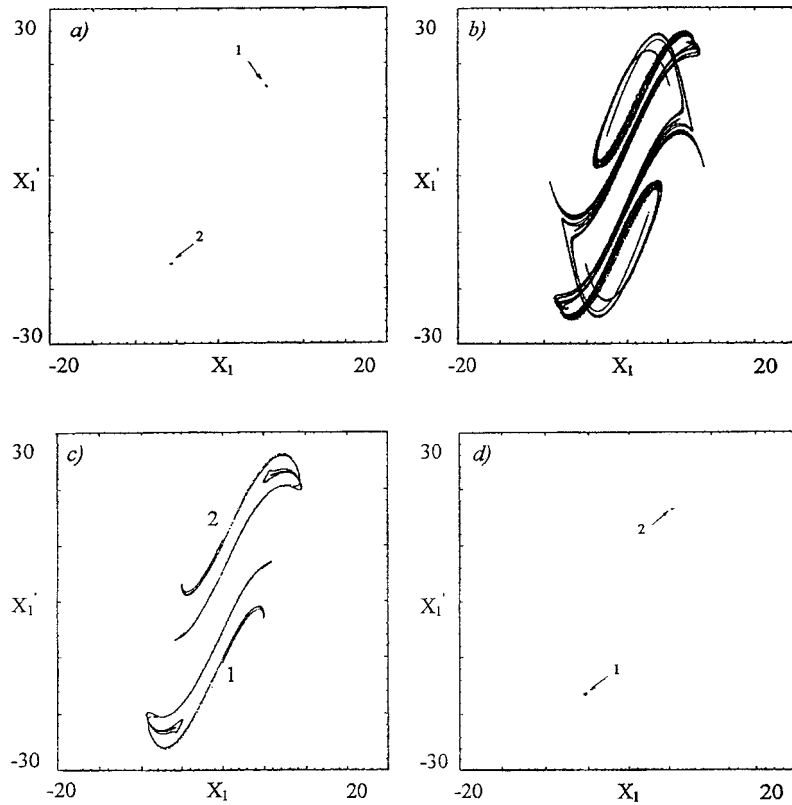


Figure 10. Poincaré maps for various values of ϑ . (a) $\vartheta = 0.98$; (b) $\vartheta = 0.1.40$; (c) $\vartheta = 1.50$; (d) $\vartheta = 1.70$.

Table 2. Lyapunov exponents for various ϑ parameters.

| ϑ | Attractor type (see Figures 10a–d) | λ_1 | λ_2 | λ_3 | λ_4 |
|-------------|---------------------------------------|-------------|-------------|-------------|-------------|
| 0.98 | Periodic – No. 1, 2 | -0.603 | -0.883 | -1.143 | -1.596 |
| 1.40 | Chaotic | 0.179 | -0.422 | -0.617 | -1.746 |
| 1.50 | Chaotic | 0.141 | -0.509 | -0.623 | -1.524 |
| 1.70 | Periodic | -0.991 | -0.912 | -0.913 | -2.444 |

coincide with the regions of positive Lyapunov exponents (Figure 9). This also confirms the results obtained by means of a Poincaré map (Figure 10).

6. Transition to Hyperchaos

It is well known that chaotic vibration of coupled oscillators can be realised in different ways depending on the analysed system parameters [10–13]. A hyperchaotic solution, defined as one which possesses more than one positive Lyapunov exponent, can appear [12, 13] particularly for multi-degrees-of-freedom systems. In this section we present possibility of hyperchaos in our model with two coupled van der Pol oscillators and with parametric

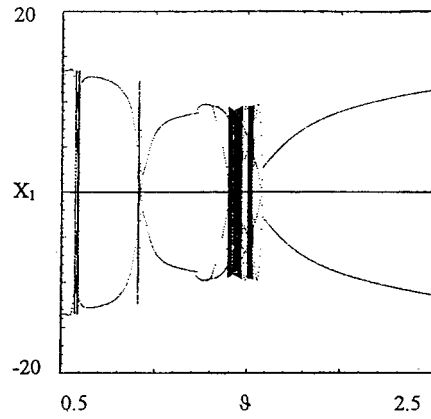


Figure 11. Bifurcation diagram versus ϑ parameter.

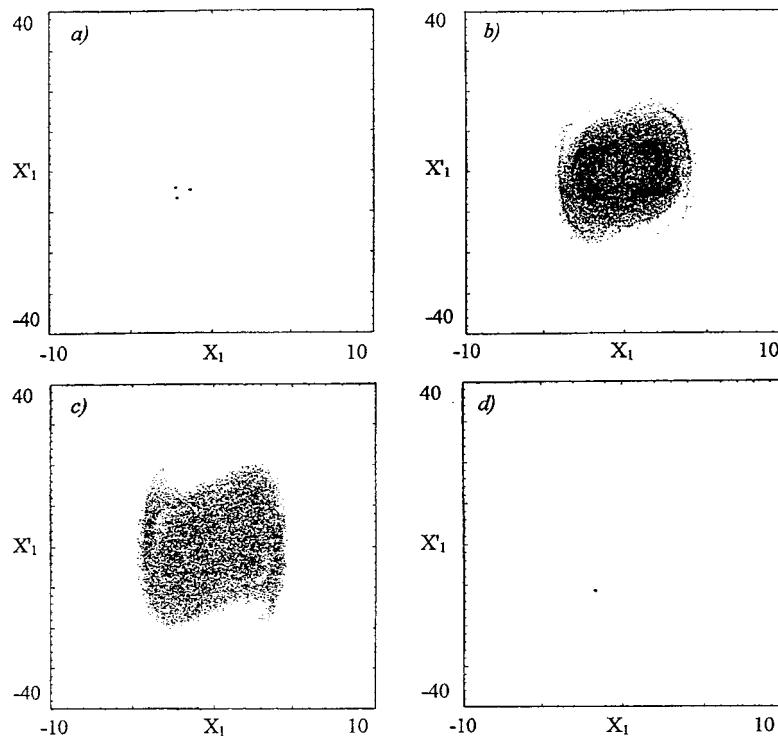


Figure 12. Poincaré maps for $\vartheta = 2.6$ and various μ (a) $\mu = 6.2$; (b) $\mu = 7.0$; (c) $\mu = 10.0$; (d) $\mu = 14.0$.

excitation. Poincaré maps for chosen system parameters: $\alpha_1 = 0.1$, $\beta_1 = 0.05$, $\gamma_1 = 3.0$, $\delta_1 = -0.5$, $\delta_2 = -0.3$, $M = 0.5$, $\vartheta = 2.6$ and various values of the excitation amplitude $\mu = 6.2, 7.0, 10.0, 14.0$ are presented in Figures 12a, 12b, 12c and 12d, respectively.

Figure 12a presents the periodic solution with three characteristic points on a Poincaré map. They correspond to a solution with a triple period of oscillation. We checked that, for larger values of μ , the solution evaluates through Hopf bifurcation to a chaotic solution

Table 3. Lyapunov exponents for various μ parameters.

| μ | Attractor type (see in Figures 12a–12d) | λ_1 | λ_2 | λ_3 | λ_4 |
|-------|--|-------------|-------------|-------------|-------------|
| 6.2 | Periodic | -0.022 | -0.022 | -0.031 | -0.031 |
| 7.0 | Hyperchaotic | 0.432 | 0.120 | -0.183 | -0.494 |
| 10.0 | Hyperchaotic | 0.536 | 0.181 | -0.261 | -0.633 |
| 14.0 | Periodic | -0.106 | -0.108 | -0.130 | -0.131 |

(Figures 12b and 12c). For a large enough value of μ , the system solution transits back to a periodic vibration with a single frequency represented by one point on the Poincaré map.

After consideration of the chaotic solution nature (Figures 12b and 12c) it appeared that two of the Lyapunov exponents were positive (Table 3). In such cases, the system manifests hyperchaotic vibration. Examples of the time histories for different types of vibrations are presented in Figures 13a–13d. Figure 13a shows the results for a chaotic solution (the system parameters as in Figure 7e).

In Figures 13b and 13c, the time histories of quasi-periodic solutions are shown with parameters corresponding to Figures 7h and 7j, respectively. Figure 13d presents the time history of hyperchaotic motion with two positive Lyapunov exponents (see Table 2). The parameters are chosen as in Figure 10c.

The difference between chaotic (Figure 13a) and quasi-periodic solutions (Figures 13b and 13c) is significant. Moreover, one can also notice the different characters of chaotic (Figure 13a) and hyperchaotic (Figure 13d) vibrations. In the case of hyperchaotic vibrations, the system seems to move differently in the sequences of time intervals. The time histories for two different quasi-periodic solutions with one (Figure 13b) or two (Figure 13c) nodal Lyapunov exponents are very similar to each other.

7. Summary and Conclusions

In this paper we have investigated the complex system of coupled non-linear oscillators excited parametrically. As usual, the interaction between self-excited and parametric excitation leads to a number of interesting results like entrainment of frequency and synchronisation phenomena. We have demonstrated that in our system for some sets of parameters, one of the main parametric resonances close to the free vibration frequency can be forbidden. Analytical methods enabled us to examine the system for small values of the μ parameter. Other interesting phenomena, like transition to chaos and hyperchaos, were detected numerically for larger values of this parameter where analytical methods are not applicable. We have examined bifurcations by means of Poincaré maps and Lyapunov exponents and found that Hopf bifurcations play a major role in this system. Different types of motion were obtained: periodic, quasi-periodic first type (closed curve on the Poincaré map), quasi-periodic second type (torus on the Poincaré map), chaotic and hyperchaotic. Transition from chaotic to hyperchaotic motion is possible in the system for larger values of the parametric excitation amplitude which, however, do not correspond to any real mechanical system. The transition from a regular to hyperchaotic solution for generalised van der Pol equations was earlier ex-

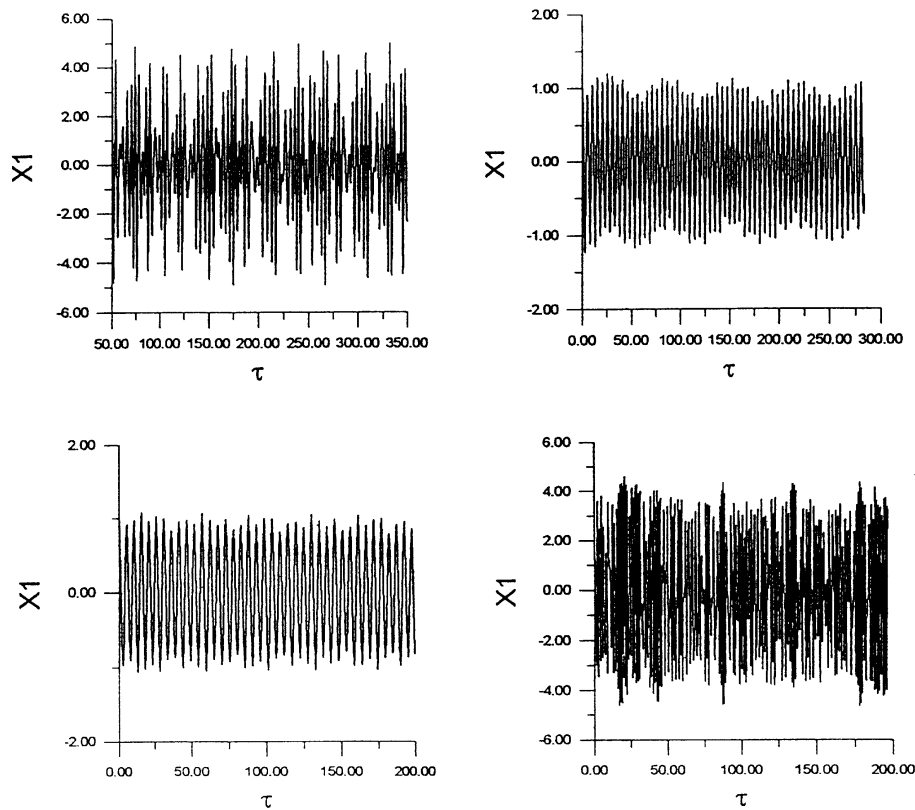


Figure 13. Vibration time histories in generalised coordinates for: (a) chaotic $\vartheta = 1.40$; (b) quasi-periodic $\vartheta = 1.80$; (c) quasi-periodic $\vartheta = 2.50$; (d) hyperchaotic $\vartheta = 2.60$.

amined by Kapitaniak and Steeb [13]. In their treatment, the model was different. It possessed no linear spring term and was subjected to an external excitation instead of a parametric one. In spite of this, the results concerning hyperchaotic vibrations we obtained are similar to theirs. The mechanism of the transition to hyperchaos in our case is still under consideration and the results will be published separately. This paper is a continuation of papers [4, 5], where the authors carried out a detailed analysis of a parametrically excited van der Pol oscillator with one degree of freedom for both regular and chaotic solutions.

References

1. Tondl, A., *On the Interaction between Self-Excited and Parametric Vibrations*, Monographs and Memoranda, Vol. 25, National Research Institute for Machine Design, Prague, 1978.
2. Yano, S., 'Considerations on self- and parametrically excited vibrational systems', *Ingenieur-Archiv* **59**, 1989, 285–295.
3. Szabelski, K. and Warmański, J., 'The non-linear vibrations of parametrically self-excited system with two degrees of freedom under external excitation', *Nonlinear Dynamics* **14**, 1997, 23–36.
4. Litak G., Szabelski, K., Spuz-Szpos, G., and Warmański, J., 'Vibration analysis of a self-excited system with parametric forcing and nonlinear stiffness', *International Journal of Bifurcation and Chaos* **9**, 1999, 493–504.
5. Szabelski, K., Litak, G., Warmański, J., and Spuz-Szpos, G., 'Vibrations synchronization and chaos in parametrically self-excited system with non-linear elasticity', in *Proceedings of EUROMECH – 2nd European*

- Nonlinear Oscillation Conference*, Prague, September 9–13, 1996, Vol. 1, L. Pust and F. Peterka (eds.), Czech Technical University, 1996, pp. 435–439.
6. Szabelski, K. and Warmiński, J., ‘The parametric self excited non-linear system vibrations analysis with the inertial excitation’, *International Journal of Non-Linear Mechanics* **30**, 1995, 179–189.
 7. Szabelski, K. and Warmiński, J., ‘The self excited system vibrations with the parametric and external excitations’, *Journal of Sound and Vibration* **908**, 1995, 595–607.
 8. Hayashi, Ch., *Nonlinear Oscillations in Physical Systems*, McGraw-Hill, New York, 1964.
 9. Litak G., Spuz-Szpos, G., Szabelski, K., and Warmiński, J., ‘Vibration of externally forced Froude pendulum’, *International Journal of Bifurcation and Chaos* **9**, 1999, 561–570.
 10. Kapitaniak, T. and Chua, L. O., ‘Locally-intermingled basins of attraction in coupled Chua’s circuits’, *International Journal of Bifurcation and Chaos* **6**, 1996, 357–366.
 11. Kapitaniak, T., ‘Transition to chaos in chaotically forced coupled oscillators’, *Physical Review* **E47**, 1993, R2975–R2978.
 12. Kapitaniak, T. and Chua, L. O., ‘Hyperchaotic attractors of unidirectionally-coupled Chua’s circuits’, *International Journal of Bifurcation and Chaos* **4**, 1994, 477–482.
 13. Kapitaniak T. and Steeb, W., H., ‘Transition to hyperchaos in coupled generalized Van der Pol’s equations’, *Physics Letters* **A152**, 1991, 33–37.
 14. Nayfeh, A. H. and Mook, D. T., *Nonlinear Oscillations*, Wiley, New York, 1979.
 15. Wiercigroch, M., ‘Chaotic vibrations of a simple model of the machine tool-cutting process system’, *Journal of Vibration and Acoustics* **119**, 1997, 468–475.
 16. Kahraman, A. and Blankenship, G. W., ‘Experiments on nonlinear dynamic behaviour of an oscillator with clearance and periodically time varying parameters’, *Journal of Applied Mechanics* **64**, 1997, 217–226.
 17. Schmidt, G., ‘Interaction of self-excited, forced and parametrically excited vibrations’, in *Applications of the Theory of Nonlinear Oscillations – The 9th International Conference on Non-Linear Oscillations*, Naukova Dumka, Kiev, 1984, pp. 310–315.
 18. Schmidt, G. and Tondl, A., *Non-Linear Vibrations*, Akademie-Verlag, Berlin, 1986.
 19. Nusse, H. E. and Yorke, J. A., *Dynamics: Numerical Explorations*, Springer-Verlag, New York, 1994.
 20. Hassard, B. D., Kazarinoff, N. D., and Wan, Y. H., *Theory and Applications of Hopf Bifurcation*, Cambridge University Press, Cambridge, 1981.